Scientia Iranica B (2011) 18 (3), 423–431

Sharif University of Technology

Scientia Iranica

Transactions B: Mechanical Engineering

www.sciencedirect.com

Research note

Synthesis of multiple-type classification algorithms for robust heart rhythm type recognition: Neuro-svm-pnn learning machine with virtual QRS image-based geometrical features

M.R. Homaeinezhad [a,b,*], E. Tavakkoli [a,b], S.A. Atyabi [a,b], A. Ghaffari [a,b], R. Ebrahimpour [c,d]

[a] *Department of Mechanical Engineering, K.N. Toosi University of Technology, Tehran, P.O. Box 19395-1999, Iran*

[b] *CardioVascular Research Group (CVRG), K.N. Toosi University of Technology, Tehran, P.O. Box 19395-1999, Iran*

[c] *Brain and Intelligent Systems Research Lab, Department of Electrical Engineering, Shahid Rajaee University, Tehran, P.O. Box 19395-5746, Iran*

[d] *School of Cognitive Sciences (SCS), Institute for Research in Fundamental Sciences (IPM), Tehran, P.O. Box 19395-5746, Iran*

Received 31 July 2010; revised 30 January 2011; accepted 1 May 2011

KEYWORDS

Feature extraction;
Curve length method;
Support vector machine;
Probabilistic neural network;
Multi layer perceptron;
Fusion (hybrid) classification;
Arrhythmia classification;
Supervised learning machine.

Abstract The paper addresses a new QRS complex, geometrical feature extraction technique, as well as its application in supervised electrocardiogram (ECG) heart-beat hybrid (fusion) classification. To this end, after detection and delineation of the major events of an ECG signal via an appropriate algorithm, each QRS region and also its corresponding Discrete Wavelet Transform (DWT) are supposed as virtual images, and each one is divided into eight polar sectors. Then, the curve length of each excerpted segment is calculated and used as an element of the feature space. To increase the robustness of the proposed classification algorithm versus noise, artifacts and arrhythmic outliers, a fusion structure consisting of four different classifiers, namely Support Vector Machine (SVM), Probabilistic Neural Network (PNN) and two Multi Layer Perceptron-Back Propagation (MLP-BP), with different topologies, were designed. To show the merit of the new proposed algorithm, it was applied to all MIT-BIH arrhythmia database records, and the discriminative power of the classifier in isolation of different beat types of each record was assessed. As a result, the average accuracy value, Acc = 98.18%, was obtained. Also, the proposed method was applied to 8 arrhythmias and an average value of Acc = 97.37% was achieved.

1. Introduction

Signal processing and data mining tools have been developed to enhance computational capabilities, in order to help clinicians in diagnoses and treatment. The electrocardiogram (ECG) is a representative signal containing information about the condition of the heart. The shape and size of the P-QRS-T wave and the time intervals between various peaks contain useful information about the nature of the disease afflicting the heart. However, a human observer cannot directly monitor these subtle details. Besides, since bio signals are highly subjective, the symptoms may appear at random in the timescale. The presence of cardiac abnormalities is generally reflected in the shape of the ECG waveform and heart rate. Therefore, study of the ECG pattern and heart rate variability has to be carried out over extended periods of time [1]. Based on a comprehensive literature survey among much documented work, it is seen that several features and extraction (selection) methods have been created and implemented by authors. For example, preprocessed ECG signals, via appropriately defined and implemented transformations, such as Discrete Wavelet Transform (DWT), Continuous Wavelet Transform (CWT) [2], Hilbert Transform (HT) [3], Fast Fourier Transform (FFT) [4,5], Short Time Fourier Transform (STFT) [6], Power Spectral Density (PSD) [7,8], higher order spectral methods [9,10], statistical moments [11], and nonlinear transformations, such as Liapunov exponents and fractals [12–14], have been used as appropriate sources for feature extraction. In order to extract feature(s) from a selected source, various methodologies and techniques have been

* Corresponding author at: Department of Mechanical Engineering, K.N. Toosi University of Technology, Tehran, P.O. Box 19395-1999, Iran.
E-mail address: mrhomaeinezhad@kntu.ac.ir (M.R. Homaeinezhad).

1026-3098 © 2011 Sharif University of Technology. Production and hosting by Elsevier B.V. Open access under CC BY-NC-ND license.
Peer review under responsibility of Sharif University of Technology.

doi:10.1016/j.scient.2011.05.033

Production and hosting by Elsevier

List of abbreviations

PNN	Probabilistic neural networks
SVM	Support vector machine
ECG	Electrocardiogram
DWT	Discrete wavelet transforms
ANN	Artificial neural network
MEN	Maximum epochs number
NHLN	Number of hidden layer neurons
RBF	Radial basis function
MLP-BP	Multi-layer perceptron back propagation
TP	True positive
P+	Positive predictivity (%)
Se	Sensitivity (%)
MITDB	MIT-BIH arrhythmia database
FIR	Finite-duration impulse response
LBBB	Left bundle branch block
RBBB	Right bundle branch block
PVC	Premature ventricular contraction
APB	Atrial premature beat
F	Fusion of ventricular and normal beat
VE	Ventricular escape beat
VF	Ventricular flutter wave
PB	Paced beat.

introduced. To meet this end, the first step is segmentation and excerption of specific parts of the preprocessed trend (for example, in the area of the heart arrhythmia classification, ventricular depolarization regions are the most used segments). Afterwards, appropriate and efficient features can be calculated from excerpted segments, via a useful method. Up to now, various techniques have been proposed for the computation of feature(s). For example, mean standard deviation, maximum to minimum value ratios, maximum–minimum slopes, summation of point to point differences, area, duration of events, correlation coefficient with a pre-defined waveform template, statistical moments of the auto (cross) correlation functions with a reference waveform [15], bi-spectrum [9], nonlinear integral transforms and some other more complicated structures [16–28] may be used as instruments for the calculation of features.

After generation of the feature source segmentation, feature selection and extraction (calculation), the resulted feature vectors should be divided into two groups: "train" and "test", to tune an appropriate classifier, such as a neural network, support vector machine or ANFIS (adaptive neuro fuzzy inference system) systems [29–36], as well as differential entropy-based intelligent techniques [37]. As previous research shows, occurrence of arrhythmia(s) affects the RR-tachogram and Heart Rate Variability (HRV) in such a way that these quantities can be used as good features to classify several rhythms. By using the RR-tachogram or HRV analysis for feature extraction, some recognition strategies, based on heuristic "IF $\cdots$ THEN" inference structures or other parametric/nonparametric classification rules [38–40], artificial neural networks, support vector machines [41] and probabilistic frameworks, such as Bayesian hypotheses tests [42], the arrhythmia classification would be fulfilled with acceptable accuracy. Traditionally, in the studies based on morphology and wave geometry, first, during a preprocessing stage, some corrections, such as baseline wander removal, noise-artifact rejection and suitable scaling, are applied. Then, using an appropriate mapping, for instance, filter banks, discrete or continuous wavelet transforms in different

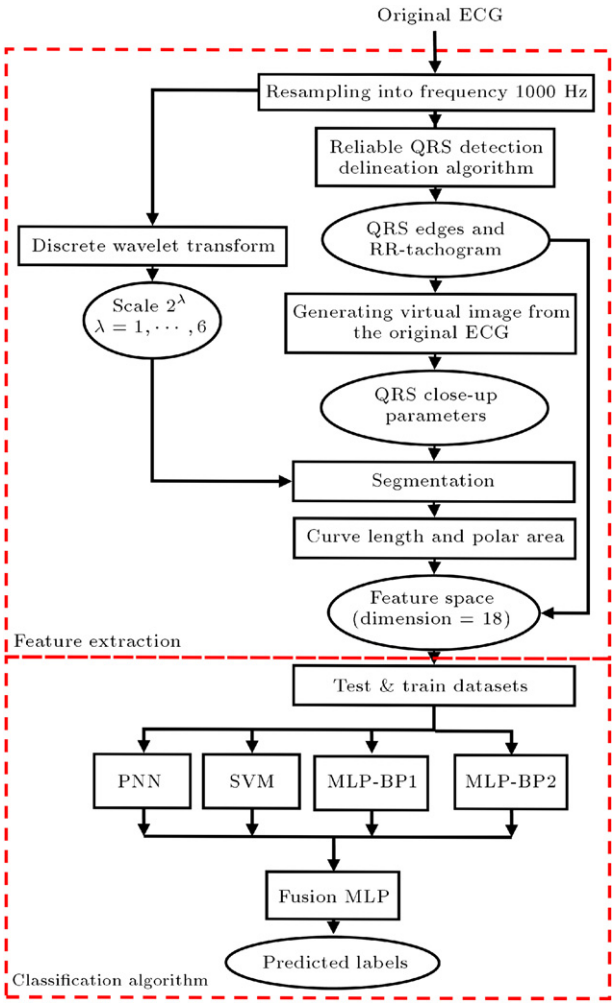

Figure 1: The general block diagram of an ECG beat type recognition algorithm supplied with virtual image-based geometrical features.

spatial resolutions etc., more information is derived from the original signal for further processing and analyses. In the area of nonlinear systems theory, some ECG arrhythmia classification methods, on the basis of fractal theory [23,24], state-space, trajectory space, phase space, Liapunov exponents [25–27] and nonlinear models [28], have been innovated by researchers. The general block diagram of the proposed heart arrhythmia recognition-classification algorithm, including a two stage train and test, is shown in Figure 1. According to this figure, first, the events of the ECG signal are detected and delineated using a robust wavelet-based algorithm [43,44]. Then, each QRS region and also its corresponding DWT are supposed as virtual images, and each of them is divided into eight polar sectors. Next, the curve length of each excerpted segment is calculated and used as an element of the feature space. To increase the robustness of the proposed classification algorithm versus noise, artifacts and arrhythmic outliers, a fusion structure consisting of four different classifiers, namely, SVM, PNN and two MLP-BP neural networks with different topologies, were designed and implemented. The new proposed algorithm was applied to all 48 records of the MIT-BIH Arrhythmia Database (MITDB) and the average value of Acc = 98.18% was obtained. Also, the proposed hybrid classifier was applied to 8 arrhythmias (Normal, LBBB, RBBB, PVC, F, VE, PB, VF) belonging to 32 MITDB, and the average value of Acc = 97.37% was achieved.

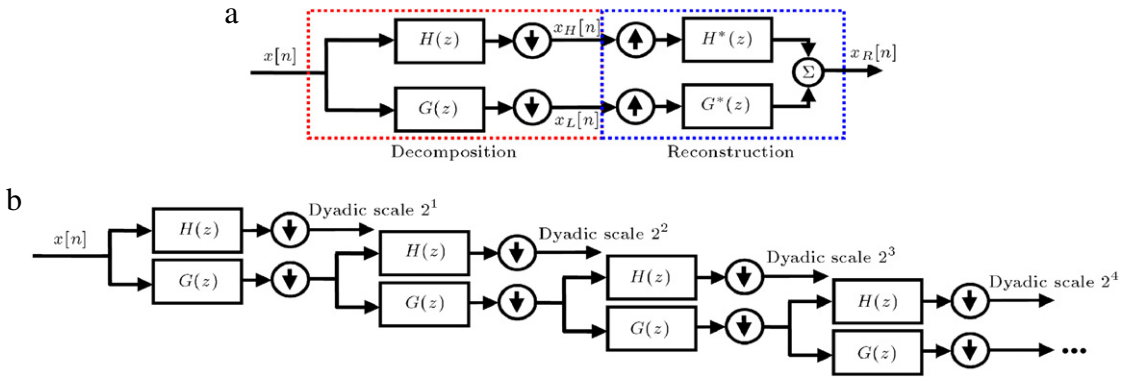

Figure 2: FIR filter-bank implementation to generate discrete wavelet dyadic scales and smoothing functions transform based on à trous algorithm. (a) One-step generation of detailed coefficient scales and reconstruction of the input signal; and (b) four-step implementation of DWT for extraction of dyadic scales.

2. Materials and methods

2.1. Discrete wavelet transform (DWT)

Generally, it can be stated that the wavelet transform is a quasi-convolution of the hypothetical signal, $x(t)$, and the wavelet function, $\psi(t)$, with dilation parameter, a, and translation parameter, b, as the following integration:

$$W_{a^x}(b) = \frac{1}{\sqrt{a}} \int_{-\infty}^{+\infty} x(t)\psi\left((t-b)/a\right) \mathrm{d}t, \quad a > 0. \tag{1}$$

Parameter a can be used to adjust the wideness of the basis function and, therefore, the transform can be adjusted in several temporal resolutions. In Eq. (1), for dilation parameter "a" and the translation parameter "b", the values $a = q^k$ and $b = q^k lT$ can be used in which q is the discretization parameter, l is a positive constant, k is the discrete scale power and T is the sampling period. By substituting the new values of parameters "a" and "b" into the wavelet function, $\psi(t)$, the following result is obtained:

$$\psi_{k,l}(t) = q^{-k/2}\psi(q^{-k}t - lT), \quad k, l \in Z^+. \tag{2}$$

Scale index k determines the width of the wavelet function, while parameter l provides a translation of the wavelet function.

If scale factor a and translation parameter b are chosen as $q = 2$, i.e. $a = 2^k$ and $b = 2^k l$, a dyadic wavelet with the following basis function will be resulted [45]:

$$\psi_{k,l}(t) = 2^{-k/2}\psi(2^{-k}t - lT), \quad k, l \in Z^+. \tag{3}$$

For a prototype wavelet, $\psi(t)$, with the following quadratic spline Fourier transform:

$$\Psi(\Omega) = j\Omega \left(\frac{\sin(\Omega/4)}{\Omega/4}\right)^4. \tag{4}$$

Transfer functions $H(z)$ and $G(z)$ (see Figure 2) can be obtained from the following equation:

$$H(\mathrm{e}^{j\omega}) = \mathrm{e}^{j\omega/2}\left(\cos(\omega/2)\right)^3,$$
$$G(\mathrm{e}^{j\omega}) = 4j\mathrm{e}^{j\omega/2}\left(\sin(\omega/2)\right). \tag{5}$$

One of the most prominent advantages of the à trous algorithm is the approximate independency of its results from a sampling frequency. This is because the main frequency content of the ECG signal concentrates on a range less than 20 Hz [43,44]. After examination of various databases with different sampling frequencies (range between 136–10 kHz), it has been concluded that in low sampling frequencies (less than 750 Hz), scales 2^λ ($\lambda = 1, 2, \ldots, 5$) are usable while for sampling frequencies more than 1000 Hz, scales 2^λ ($\lambda = 1, 2, \ldots, 8$) contain profitable information that can be used for the purpose of wave detection, delineation and classification.

2.2. Probabilistic neural network

A probabilistic neural network is a kind of radial basis network that can be used for classification problems. Training of a probabilistic neural network is much easier than for back propagation. It can be simply finished by setting the weights of the network using the training set. When an input is presented, the first layer computes distances from the input vector to the training input vectors, and produces a vector whose elements indicate how close the input is to a training input. The second layer sums up these contributions for each class of input, to produce, as its net output, a vector of probabilities. Finally, a complete transfer function on the output of the second layer picks the maximum of these probabilities, and produces 1 for that class and 0 for the other class.

2.3. Radial basis function based support vector machine (RBF–SVM) classifier

Special forms of ANNs are SVMs, introduced by Boser, Guyon and Vapnik, in 1992. SVM's perform classification by non-linearly mapping their n-dimensional input into a high dimensional feature space. In this high dimensional feature space, a linear classifier is constructed. Explicit mapping would be computationally unreasonable, and the algorithm avoids that by introducing the kernel, which is possible, since the algorithm only uses the scalar product of the inputs. From this, the classification problem is translated into a convex quadratic optimization problem, which, due to its convexity, has a unique solution. More details about fundamental concepts of SVM can be found in [46].

3. Neuro-SVM–PNN fusion classification algorithm: Design, implementation and performance evaluation

3.1. QRS geometrical features extraction

3.1.1. ECG events detection and delineation

In this step, QRS complexes are detected and delineated. Today, reliable QRS detectors, based on Hilbert [47,48] and Wavelet [43,44] transforms, can be found in literature. In this study, an ECG detection-delineation method is introduced,

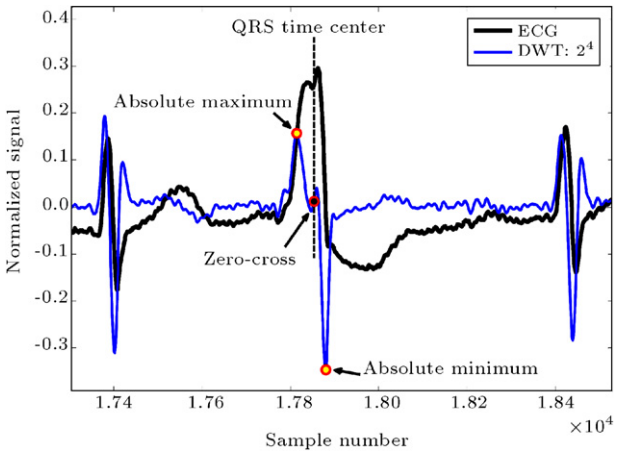

Figure 3: Determination of the time center of a detected QRS complex using excerpted DWT scale 2^4.

with sensitivity and positive predictivity (Se = 99.95% and P+ = 99.94%), and average maximum delineation errors of 6.1 m s, 4.1 m s and 6.5 m s are implemented for P-wave, QRS complex and T-wave, respectively [43]. By application of this method, detecting the major characteristic locations of each QRS complex, i.e. fiducial, *R* and *J* locations, becomes possible.

3.1.2. Detected QRS complex geometrical features extraction [49]

In order to compute features from the detected QRS complexes, either normal or arrhythmic, via the proposed method, first, a reliable time center should be obtained for each QRS complex. To find this point, the absolute maximum and minimum indices of the excerpted DWT dyadic scale, 2^4, using the onset–offset locations of the corresponding QRS complex, are determined. It should be noted that according to comprehensive studies fulfilled in this research, the best time center of each detected QRS complex is the mean of the zero-crossing locations of the excerpted DWT (see Figure 3).

To make a virtual close-up from each detected QRS complex, a rectangle is built on the complex with the following specifications:

- The left-side mid-span of the rectangle is the fiducial location of the QRS complex.
- The absolute distance of the complex from the fiducial point is half of the rectangle height.
- The center of the rectangle is the time-center of the QRS complex.
- The right-hand abscissa of the rectangle is the distance between the QRS time center and its *J*-location.

Afterwards, each QRS region and also its corresponding DWT are supposed as virtual images, and each of them is divided into eight polar sectors. Next, the curve length of each excerpted segment is calculated and used as elements of the feature space (therefore, for each detected QRS complex, 16 features are computed). The quantity curve-length of a hypothetical time series, $x(t)$, in a window with length W_L samples, can be estimated as:

$$M_{CL}(k) \approx \frac{1}{F_s} \sum_{t=k}^{k+W_L-1} \sqrt{1 + [(x(t+1) - x(t))\, F_s]^2}, \qquad (6)$$

where F_s the is sampling frequency of the time series, $x(t)$. The curve length is suitable for measuring the duration of the signal, $x(t)$, events being either strong or weak. Generally, the M_{CL} measure indicates the extent of flatness (smoothness or impulsive peaks) of samples in the analysis window. This

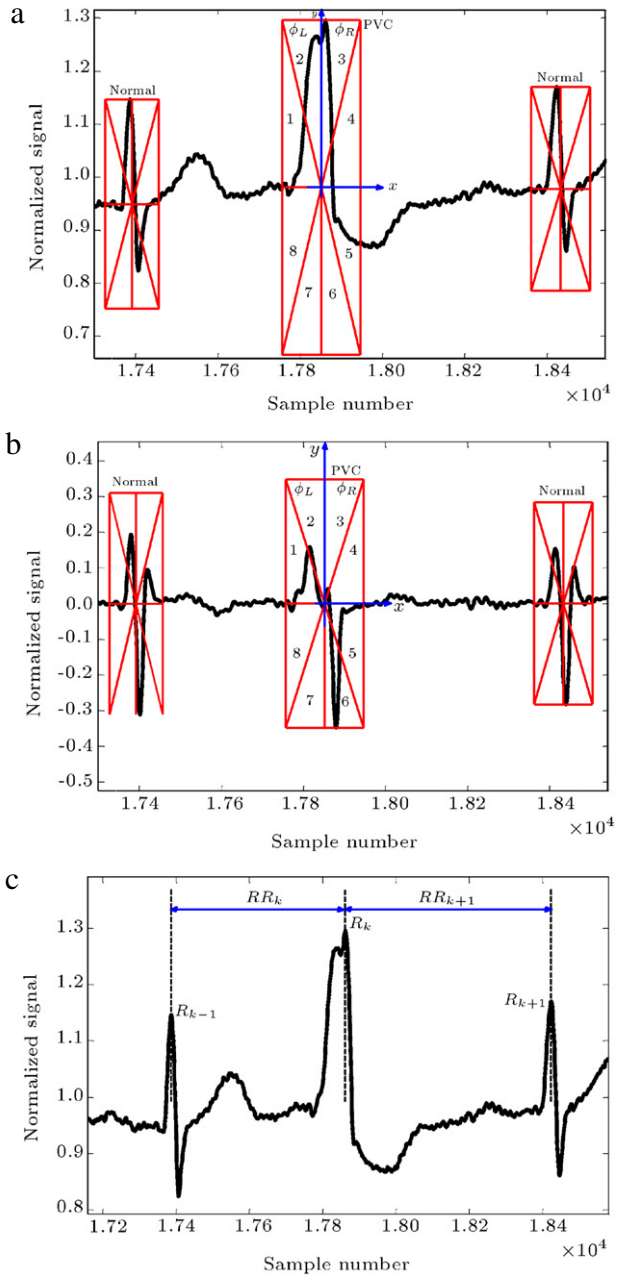

Figure 4: Extraction of geometrical features from a delineated QRS complex via segmentation of each complex into 8 polar sectors by generating a virtual image from the complex. (a) Original ECG; (b) DWT of the original ECG; and (c) RR-interval.

measure allows the detection of sharp ascending/descending regimes occurred in the excerpted segment [44].

A generic example of a Holter ECG and its corresponding 2^4 DWT dyadic scale, with the virtual images of the complexes provided for feature extraction, as well as two quantities obtained from the RR-tachogram, are shown in Figure 4.

3.2. Design of the hybrid (fusion) neuro-SVM–PNN classification algorithm

3.2.1. Design of the particle classifiers

In the heart-beat classification context, due to differences existing in the theory and structure of the several types

of classifier, such as Artificial Neural Network (ANN), PNN and SVM, reasonably achieving exactly similar results from them, given a common train and test feature spaces cannot be expected. In order to increase the total accuracy of the proposed classification algorithm, one way is to synthesize the output of several classification algorithms with different inherent structures to achieve the best accuracy, as much as possible, leading to higher robustness against uncertainties and probable arrhythmia or outliers. In this study, to build a fusion (hybrid) classification scheme, four types of different classification methods, namely, SVM, PNN, and two MLP-BP with different topologies, are properly regulated using the train dataset. The specifications of each classification algorithm are described below.

- *SVM classifier*. Each SVM includes two parameters, C and γ, that should be tuned properly to attain satisfactory accuracy. In this study, the best choices for parameters C and γ were concluded to be 10 and 0.000001, respectively. The predicted labels of the input feature vector were considered as the output of this classifier in the fusion structure.
- *PNN classifier*. As mentioned previously in Section 2.2, this classifier has two layers. For this topology, the parameter of spread is chosen to be 100.
- *MLP-BP*1. The first MLP-BP classifier includes one hidden layer with a Number of Hidden Layer Neurons (NHLN) equal to 17, and the tangent sigmoid and the logarithmic sigmoid as the activation functions of the hidden layer and output layer, respectively. Also, for this ANN, MEN is chosen to be 200.
- *MLP-BP*2. This classifier possesses one hidden layer with NHLN = 20. The tangent sigmoid was chosen as the activation function for both hidden and output layers, respectively. For this ANN, MEN = 300 was assigned.

It should be noticed that several parameters, such as types of activation function and several values for NHLN and MEN, were examined and altered based on the trial-and-error method, and suitable ranges and types were chosen for these parameters.

From each classifier embedded into the fusion structure, the following outputs are processed:

- Predicted labels for train and test feature space.
- Accuracy of classifier.

The predicted labels of each particle classification algorithm are used for creation of a hybrid classifier, consisting of a PNN, a SVM and two MLP-BP type ANN classifiers.

3.2.2. Neuro-SVM–PNN fusion classification scheme

To design a fusion classification algorithm, after appropriate training of the SVM, PNN and the MLP-BP classifiers, another MLP-BP network is regulated to merge results of all particle classifiers. To train this classifier, each train feature is inputted to all classifiers and the obtained labels are set as the train feature vector for the fusion network. By training a MLP-BP network to combine the outcome of each classifier, a nonlinear mapping between structural classifiers and true labels is identified, which has more generalization power than each structural classifier.

This classifier possesses one hidden layer, with NHLN = 20. The logarithmic sigmoid and tangent sigmoid were chosen as the activation functions of the hidden and output layers, respectively. For this ANN, MEN = 1000 was assigned. In Figure 5, the block diagram of the proposed fusion classification algorithm, including four different classifiers in the train and test stages, is illustrated.

Table 1: The different rhythm types and the corresponding equivalent ASCII code integer numbers.

Numeric code	Rhythm
33	Ventricular flutter wave
34	Comment annotation
43	Rhythm change
47	Paced beat
65	Atrial premature beat
69	Ventricular escape beat
70	Fusion of ventricular and normal beat
74	Nodal (junctional) premature beat
76	Left bundle branch block beat
78	Normal beat
81	Unclassifiable beat
82	Right bundle branch block beat
83	Supraventricular premature or ectopic beat
86	Premature ventricular contraction
91	Start of ventricular flutter/fibrillation
93	End of Ventricular flutter/fibrillation
97	Aberrated atrial premature beat
101	Atrial escape beat
102	Fusion of paced and normal beat
106	Nodal (junctional) escape beat
120	Non-conducted P-wave (blocked APC)
124	Isolated QRS-like artifact
126	Change in signal quality

To evaluate the performance of the proposed feature extraction method and the fusion classification algorithm, the following steps are pursued:

- Evaluation of the discriminative power of the selected features.
- Design of particle classifiers and their implementation to all MITDB records.
- Design of the fusion classifier for each MITDB record, and comparing the obtained results with each particle classifier.
- Selection of some rhythms from MITDB records and design of the particle and fusion classifiers.
- Comparison of the obtained final results with previous similar peer-reviewed studies.

3.3. Results and discussion

In Table 1, the numeric codes of the 23 MITDB rhythms and their corresponding annotations are illustrated. After implementation of the PNN, SVM and two MLP-BP neural network classifiers and the corresponding fusion classifier to all 48 MITDB records, and calculation of accuracy, the obtained results are shown in Table 2. According to this table, the fusion classifier yielded an average accuracy of Acc = 98.18%, given all data and rhythms of MITDB records. In Figure 6, a graphical illustration of Table 2 is shown. As seen in this figure, the overall performance quality associated with the fusion classification algorithm is superior rather than the structural classifiers embedded in the body of the hybrid algorithm. It should be noted that, although, in some records of the MITDB, one or some particle classifiers might have better performance compared to the fusion classifier, this behavior does not continue uniformly for all records and, therefore, the superiority of the fusion scheme is justified.

Between record classifications, 32 records are selected from MITDB records, and rhythms Normal, Left Bundle Branch Block (LBBB), Right Bundle Branch Block (RBBB), Premature Ventricular Contraction (PVC), fusion of ventricular and normal beat (F), Ventricular Escape beat (VE), Paced Beat (PB) and Ventricular Flutter wave (VF) are extracted according to the

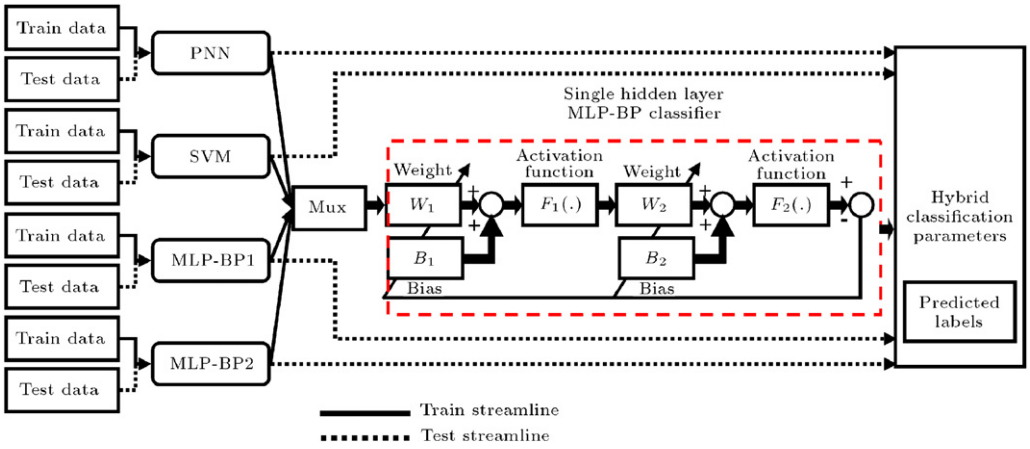

Figure 5: General block diagram of the fusion (hybrid) classification algorithm consisting of four particle classifiers, namely, PNN, SVM, classifiers, and four MLP-BP networks.

Table 2: Performance illustration of the particle classifiers SVM, PNN and two MLP-BP networks, as well as the corresponding performance of the fusion classification algorithm.

MIT Rec	Total # of beats	Rhythm codes	# of beats of each annotated rhythm	# class	SVM	PNN	1st neural net	2nd neural net	Neural net. Hybrid classifier
100	2274	[43, 78, 65, 86]	[1, 2239, 33, 1]	2	100	99.89	99.2291	98.6784	99.8203
101	1874	[43, 78, 126, 124, 81, 65]	[1, 1860, 4, 4, 2, 3]	3	99.8660	100	99.7319	99.7319	99.866
102	2192	[43, 47, 102, 78, 86]	[5, 2028, 56, 99, 4]	5	98.5126	99.54	94.6224	96.2243	98.3982
103	2091	[43, 78, 126, 65]	[1, 2082, 6, 2]	2	99.7605	100	99.8802	100	99.8802
104	2311	[43, 47, 102, 126, 81, 78, 86]	[45, 1380, 666, 37, 18, 163, 2]	6	91.6304	91.41	95.3261	95	95.6522
105	2691	[43, 78, 86, 126, 124, 81]	[1, 2526, 41, 88, 30, 5]	5	97.0177	97.86	94.3150	94.0354	97.6701
106	2098	[126, 43, 78, 86]	[30, 41, 1507, 520]	4	96.2963	95.94	96.1493	98.4468	98.3274
107	2140	[43, 47, 86, 126]	[1, 2078, 59, 2]	2	100	100	100	99.8829	97.1897
108	1824	[43, 78, 86, 120, 126, 65, 124, 70, 106]	[1, 1740, 16, 11, 41, 4, 8, 2, 1]	6	98.2044	98.89	95.3039	97.3757	98.2762
109	2535	[43, 76, 70, 86, 126]	[1, 2492, 2, 38, 2]	2	100	100	99.3076	98.5163	97.6261
111	2133	[43, 76, 126, 86]	[1, 2123, 8, 1]	2	99.6479	100	99.7653	100	99.7653
112	2550	[43, 78, 126, 65]	[1, 2537, 10, 2]	2	99.6071	100	99.6071	99.6071	99.9018
113	1796	[43, 78, 97]	[1, 1789, 6]	2	100	100	99.8605	100	99.1395
114	1890	[43, 78, 86, 74, 70, 124, 126, 65]	[3, 1820, 43, 2, 4, 1, 7, 10]	5	99.0679	99.73	99.2011	99.3342	99.4561
115	1962	[43, 78, 126, 124]	[1, 1953, 2, 6]	2	99.6169	100	99.7446	99.4891	99.7446
116	2421	[43, 78, 86, 65, 126]	[1, 2302, 109, 1, 8]	3	99.4824	99.86	99.4824	99.4824	99.4824
117	1539	[43, 78, 126, 65]	[1, 1534, 3, 1]	1	100	100	100	100	100
118	2301	[43, 82, 86, 65, 120, 126]	[1, 2166, 16, 96, 10, 12]	5	98.2552	98.36	96.7285	92.1483	94.4384
119	2094	[43, 78, 86, 126]	[103, 1543, 444, 4]	4	97.9641	99.28	99.8802	100	99.8802
121	1876	[43, 78, 126, 65, 86]	[1, 1861, 12, 1, 1]	2	100	100	99.4660	99.4660	99.4660
122	2479	[43, 78, 124]	[1, 2476, 2]	1	100	100	100	100	100
123	1519	[43, 78, 86]	[1, 1515, 3]	1	100	100	100	100	100
124	1634	[43, 82, 74, 86, 70, 65, 126, 106]	[13, 1531, 29, 47, 5, 2, 2, 5]	6	95.2160	95.67	96.9136	96.4506	95.9877
200	2792	[43, 86, 78, 65, 126, 70]	[148, 826, 1743, 30, 43, 2]	5	93.4412	93.44	95.3279	95.5975	95.9569
201	2039	[43, 78, 97, 106, 86, 120, 65, 74, 126, 70]	[35, 1625, 97, 10, 198, 37, 30, 1, 4, 2]	8	92.4598	91.71	90.1112	96.0445	97.5290
202	2146	[43, 78, 86, 65, 124, 97, 70]	[8, 2061, 19, 36, 2, 19, 1]	5	97.6581	98.36	95.6674	95.68	98.43
203	3107	[43, 126, 78, 86, 97, 124, 81, 70]	[45, 57, 2529, 444, 2, 25, 4, 1]	6	95.2342	96.36	90.4685	92.0194	97.5574
205	2672	[43, 78, 86, 65, 70, 126, 124]	[13, 2571, 71, 3, 11, 2, 1]	4	98.9662	99.25	99.1541	98.9662	99.2586
207	2385	[43, 82, 86, 76, 91, 33, 93, 126, 124, 69, 65]	[24, 86, 105, 1457, 6, 472, 6, 15, 2, 105, 107]	10	95.6660	94.58	92.0719	96.5116	96.8879
208	3040	[43, 70, 86, 78, 126, 124, 83, 81]	[53, 373, 992, 1586, 24, 8, 2, 2]	6	96.9447	93.54	93.6416	97.4401	97.0273
209	3052	[43, 78, 65, 124, 126, 86]	[21, 2621, 383, 7, 19, 1]	5	97.5349	97.7	87.8389	93.5086	98.7395
210	2685	[43, 78, 86, 70, 126, 97, 124, 69]	[17, 2423, 194, 10, 17, 22, 1, 1]	6	97.1936	97.29	95.1356	96.0804	98.6614
212	2763	[43, 82, 78, 126, 124]	[1, 1825, 923, 13, 1]	3	98.3681	98.91	94.3699	96.0789	98.9121
213	3294	[43, 78, 70, 65, 86, 97]	[43, 2641, 362, 25, 220, 3]	5	92.4600	94.97	96.1158	94.7906	95.5826
214	2297	[43, 76, 86, 126, 124, 81, 34, 70]	[25, 2003, 256, 4, 5, 2, 1, 1]	5	98.5777	99.45	95.7330	99.0153	99.2341
215	3400	[43, 78, 86, 126, 65, 34, 70]	[5, 3195, 164, 30, 3, 2, 1]	4	99.1882	99.48	93.5793	92.2509	99.7786
217	2280	[43, 47, 102, 86, 78, 126, 124]	[67, 1542, 260, 162, 244, 4, 1]	6	85.5727	86.66	95.8150	96.7621	97.1366
219	2312	[43, 78, 86, 70, 34, 65, 120]	[21, 2082, 64, 1, 4, 7, 133]	6	97.3941	97.71	98.6971	98.9142	97.9772
220	2069	[43, 78, 65, 126]	[17, 1954, 94, 4]	4	99.7576	98.54	98.3030	96.3636	99.2727
221	2462	[43, 78, 86, 126]	[23, 2031, 396, 12]	4	97.9654	98.78	98.1689	83.5198	99.0844
222	2634	[43, 78, 126, 65, 106, 74]	[136, 2062, 15, 208, 212, 1]	5	86.4762	85.33	87.0476	86.8571	87.0476
223	2643	[43, 78, 86, 65, 101, 70, 126, 97]	[28, 2029, 473, 72, 16, 14, 10, 1]	7	95.0570	92.49	98.0989	97.7186	97.8517
228	2141	[43, 78, 124, 86, 126, 65, 34]	[41, 1688, 24, 362, 20, 3, 3]	5	96.4747	95.53	76.4982	97.6498	96.5922

Table 2 (*continued*)

MIT Rec	Total # of beats	Rhythm codes	# of beats of each annotated rhythm	# class	SVM	PNN	1st neural net	2nd neural net	Neural net. Hybrid classifier
230	2466	[43, 78, 126, 124, 86]	[207, 2255, 2, 1, 1]	2	100	99.8	99.8984	100	98.8862
231	2011	[43, 82, 34, 78, 120, 65, 86]	[11, 1254, 427, 314, 2, 1, 2]	4	97.7500	99	99	99.1250	99.2500
232	1816	[43, 82, 65, 126, 106]	[1, 397, 1382, 35, 1]	3	96.2707	94.89	97.2376	96.8232	97.3757
233	3152	[43, 86, 78, 65, 70, 124]	[71, 831, 2230, 7, 11, 2]	5	97.2951	98.57	85.1233	98.9658	99.3667
234	2764	[43, 78, 126, 74, 86]	[3, 2700, 8, 50, 3]	3	99.7278	99.82	99.2740	99.6370	99.4555
Total # of subjects			48						
Average accuracy			98.1838						
Total of complexes			112, 646						

Table 3: The name of selected MITDB records with their rhythm types contents.

	Records	Training samples for each record	Testing samples for each record
Normal	100, 101, 103, 105, 112, 114, 115, 117, 121, 122, 123, 205	75	50
LBBB	109, 111, 207, 214	100	100
RBBB	118, 124, 212, 231	100	100
PVC	106, 119, 200, 203, 208, 228, 233	100	80
F	208, 213	150	100
VE	207	54	50
PB	102, 104, 107, 217	100	100
VF	207	236	200
Total		3390	2510

Table 4: Performance evaluation of the hybrid neuro-SVM–PNN classification algorithm for the selected MITDB records the confusion matrix.

	Normal	LBBB	RBBB	PVC	F	VE	PB	VF
Normal	592	3	1	3	0	0	1	0
LBBB	4	291	0	4	0	1	0	0
RBBB	0	0	294	5	1	0	0	0
PVC	6	3	4	535	6	1	3	2
F	0	0	0	7	193	0	0	0
VE	0	1	0	2	0	47	0	0
PB	1	0	0	3	0	0	296	0
VF	1	0	0	1	1	0	1	196

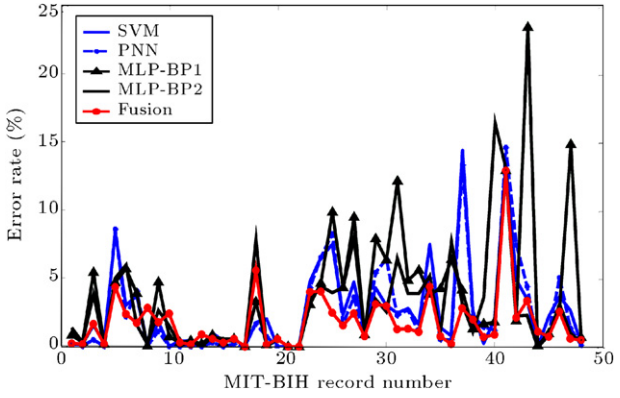

Figure 6: Error-rate percentage obtained by application of the proposed neuro-SVM–PNN fusion classification method and its structural particle classifiers to all records of the MITDB.

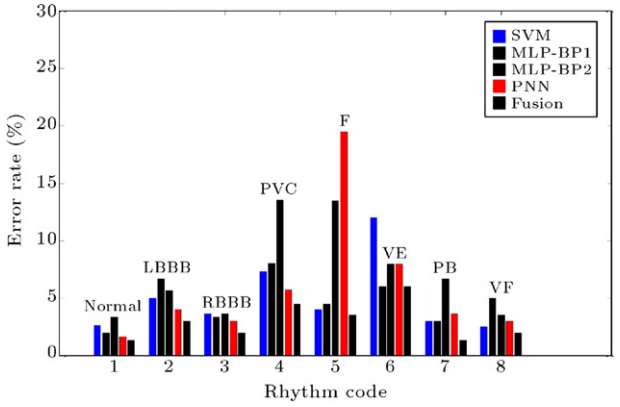

Figure 7: Error-rate diversity analysis for justification of the fusion of SVM, PNN and two MLP-BP classifiers.

MITDB annotation files. In Table 3, the names of MITDB records, as well as the selected rhythm types and their corresponding beat numbers, are presented.

3.3.1. Error analysis

It should be noted that if some diversely designed classification algorithms show error rate diversity relative to each other for a given common database, then, their utilization in a fusion classification structure is justified. In Figure 7, the error rate diversity of structural classifiers, including SVM, PNN, and two MLP-BP types, and also the proposed hybrid classifier is demonstrated. In Table 4, the performance of the fusion classification algorithm has been described by the obtained confusion matrix.

Table 5: Performance evaluation of the presented fusion classification algorithm. (a) Results obtained from several classification algorithms implemented in this study including SVM, MLP-BP, PNN and the Neuro-SVM–PNN classifiers; (b) summary of previous study.

(a) Results of this study

Classifier	Accuracy for each class (%)								Total accuracy (%)
	Normal	LBBB	RBBB	PVC	F	VE	PB	VF	
SVM	98.34	96	97	94.3	80.5	92	96.34	97	95.1
MLP-BP1	97.34	95	96.34	92.68	96	88	97	97.5	95.58
MLP-BP2	98	93.34	96.67	91.96	95.5	94	97	95	95.3
PNN	96.67	94.34	96.34	86.43	86.5	92	93.34	96.5	92.75
Fusion (Neuro-SVM–PNN)	98.67	97	98	95.54	96.5	94	98.67	98	97.37

(b) Summary of previous study

Authors	Method	Signal	Dataset	Accuracy (%)
Osowski and Linh [50]	Feature extraction: cumulants of the second, third and fourth order classification: fuzzy hybrid neural network	ECG	7185 beats from MIT-BIH; 4035 training-3150 testing [Normal: 2250, APB: 658, LBBB: 1200, PVC: 1500, RBBB: 1000, VF: 472, VE: 105]	96.06
Dokur and Olmez [51]	Feature extraction: discrete wavelet transform classification: intersecting spheres network	ECG	3000 beats from MIT-BIH; Normal, LBBB, RBBB, P, p, a, VE, PVC, F, f: 300 from each category; 1500 training-1500 testing	95.7
Hu et al. [52]	Feature extraction: PCA in 29 points from QRS, instantaneous and average RR-interval, QRS complex width classification: mixture of experts (SOM, LVQ)	ECG	25 min from each record in MIT-BIH 200 series excluding records 212, 217, 220, 222 and 232 [Normal: 43 897, PVC: 5363]	95.52
Tsipouras et al. [29]	Feature extraction: RR-interval classification: knowledge-based system	RR interval signal	30 000 beats from MIT-BIH [N, P, f, P, Q, LBBB, RBBB: 25 188, PVC, F: 2950, APB, a, J, S: 1213, e, j, n, VE: 265, VF: 384]	95.85
This study	Feature extraction: geometrical properties obtained from segmentation of each detected-delineated QRS complex virtual image as well as RR-tachogram (18 features for each detected heart beat) classification: a fusion structure consisting of SVM, PNN and two MLP-BP classifiers	ECG	5900 beats from MIT-BIH; 3390 training-2510 testing [Normal: 1500, LBBB: 700, RBBB: 700, PVC:1260, F:500, VE:104, PB:700, VF: 436]	97.37

3.4. Arrhythmia classification performance comparison with other works

The result of a comparison of the proposed method and other work [50–52] is shown in Table 5. In this table, several classification algorithms, such as MLP-BP, PNN, SVM and Probabilistic Neural Networks (PNN) are examined to determine the best elements for the final fusion classification algorithm.

4. Conclusion

In this study, a new supervised heart arrhythmia hybrid (fusion) classification algorithm, based on a new QRS complex geometrical feature extraction technique, as well as an appropriate choice from each beat RR-tachogram, was described. In the proposed method, first, the events of the ECG signal were detected and delineated using a robust wavelet-based algorithm. Then, each QRS region and also its corresponding DWT were supposed as virtual images, and each of them was divided into eight polar sectors. Next, the curve length of each excerpted segment was calculated and used as the element of the feature space. To increase the robustness of the proposed classification algorithm versus noise, artifacts and arrhythmic outliers, a fusion structure consisting of four different classifiers, namely SVM, PNN and two MLP-BP neural networks with different topologies was designed. To show the merit of the new proposed algorithm, it was applied to all 48 MITDB records and the discrimination power of the classifier, in isolation of different beat types of each record, was assessed and, as a result, the average value of Acc = 98.18% was obtained as the accuracy. Also, the proposed method was applied to 8 arrhythmias, namely, Normal, LBBB, RBBB, PVC, F, VE, PB, VF, belonging to 32 MITDB, and an average value of Acc = 97.37% was achieved showing a marginal improvement in the area of the heart arrhythmia classification. To evaluate the performance quality of the new proposed hybrid learning machine, the obtained results were compared with several similar studies.

References

[1] Acharya, U.R., *Advances in Cardiac Signal Processing*, Springer Publishing (2007).
[2] Lin, C.H., Du, Y.C. and Chen, T. "Adaptive wavelet network for multiple cardiac arrhythmias recognition", *Expert Systems with Applications*, 34, pp. 2601–2611 (2008).
[3] Benitez, D., Gaydecki, P.A., Zaidi, A. and Fitzpatrick, A.P. "The use of the Hilbert transform in ECG signal analysis", *Computers in Biology and Medicine*, 31, pp. 399–406 (2001).
[4] Christov, I., Gomez-Herrero, G., Krasteva, V., Jekova, I., Gotchev, A. and Egiazarian, K. "Comparative study of morphological and time–frequency ECG descriptors for heartbeat classification", *Medical Engineering & Physics*, 28, pp. 876–887 (2006).
[5] Lin, C.H. "Frequency-domain features for ECG beat discrimination using grey relational analysis-based classifier", *Computers and Mathematics with Applications*, 55, pp. 680–690 (2008).
[6] Tsipouras, M.G. and Fotiadis, D.I. "Automatic arrhythmia detection based on time and time–frequency analysis of heart rate variability", *Computer Methods and Programs in Biomedicine*, 74, pp. 95–108 (2004).
[7] Kar, S. and Okandan, M. "Atrial fibrillation classification with artificial neural networks", *Pattern Recognition*, 40, pp. 2967–2973 (2007).
[8] Stridh, M., Sörnmo, L., Meurling, C.J. and Olsson, S.B. "Sequential characterization of atrial tachyarrhythmia based on ECG time–frequency analysis", *IEEE Transactions on Biomedical Engineering*, 1(51), (2004).
[9] Yu, S.N. and Chen, Y.H. "Noise-tolerant electrocardiogram beat classification based on higher order statistics of sub band components", *Artificial Intelligence in Medicine*, 46, pp. 165–178 (2009).
[10] Khadra, L., Al-Fahoum, A.S. and Binajjaj, S. "A quantitative analysis approach for cardiac arrhythmia classification using higher order spectral techniques", *IEEE Transactions on Biomedical Engineering*, 11(52), pp. 1234–1246 (2005).

[11] de Chazal, P., O'Dwyer, M. and Reilly, R.B. "Automatic classification of heartbeats using ECG morphology and heartbeat interval features", *IEEE Transactions on Biomedical Engineering*, 7(51), pp. 158–171 (2004).
[12] Nopone, K., Kortelainen, J. and Seppanen, T. "Invariant trajectory classification of dynamical systems with a case study on ECG", *Pattern Recognition*, 42, pp. 1832–1844 (2009).
[13] Povinelli, R.J., Johnson, M.T., Lindgren, A.C., Roberts, F.M. and Ye, J. "Statistical models of reconstructed phase spaces for signal classification", *IEEE Transactions on Signal Processing*, 6(54), pp. 897–913 (2006).
[14] Owis, M.I., Abou-Zied, A.H., Youssef, A.M. and Kadah, Y.M. "Study of features based on nonlinear dynamical modeling in ECG arrhythmia detection and classification", *IEEE Transactions on Biomedical Engineering*, 7(49), pp. 756–764 (2002).
[15] Minhas, F.A. and Arif, M. "Robust electrocardiogram (ECG) beat classification using discrete wavelet transform", *Physiological Measurement*, 29, pp. 555–570 (2008).
[16] Chudacek, V., Georgoulas, G., Lhotska, L., Stylios, C., Petrık, M. and Cepek, M. "Examining cross-database global training to evaluate five different methods for ventricular beat classification", *Physiological Measurement*, 30, pp. 661–677 (2009).
[17] Exarchos, T.P., Tsipouras, M.G., Exarchos, C.P., Papaloukas, C., Fotiadis, D.I. and Michalis, L.K. "A methodology for the automated creation of fuzzy expert systems for ischemic and arrhythmic beat classification based on a set of rules obtained by a decision tree", *Artificial Intelligence in Medicine*, 40, pp. 187–200 (2007).
[18] Christov, I. and Bortolan, G. "Ranking of pattern recognition parameters for premature ventricular contractions classification by neural networks", *Physiological Measurement*, 25, pp. 1281–1290 (2004).
[19] Polat, K., Kara, S., Güven, A. and Günes, S. "Usage of class dependency based feature selection and fuzzy weighted pre-processing methods on classification of macular disease", *Expert Systems with Applications*, 36, pp. 2584–2591 (2009).
[20] Liu, H., Sun, J., Liu, L. and Zhang, H. "Feature selection with dynamic mutual information", *Pattern Recognition*, 42, pp. 1330–1339 (2009).
[21] Abe, N. and Kudo, M. "Non-parametric classifier-independent feature selection", *Pattern Recognition*, 39, pp. 737–746 (2006).
[22] Peng, H., Long, F. and Ding, C. "Feature selection based on mutual information: criteria of max-dependency, max-relevance, and min-redundancy", *IEEE Transactions on Pattern Analysis and Machine Intelligence*, 8(27), pp. 1413–1426 (2005).
[23] Lin, C.H., Du, Y. and Chen, T. "Nonlinear interpolation fractal classifier for multiple cardiac arrhythmias recognition", *Chaos, Solitons and Fractals*, 42, pp. 2570–2581 (2009).
[24] Wang, Y., Zhu, Y., Thakor, N.V. and Xu, Y. "A short-time multifractal approach for arrhythmia detection based on fuzzy neural network", *IEEE Transactions on Biomedical Engineering*, 9(48), pp. 924–931 (2001).
[25] Rohani Sarvestani, R., Boostani, R. and Roopaei, M. "VT and VF classification using trajectory analysis", *Nonlinear Analysis: Theory, Methods & Applications*, 71(12), pp. 55–61 (2009).
[26] Nopone, K., Kortelainen, J. and Seppanen, T. "Invariant trajectory classification of dynamical systems with a case study on ECG", *Pattern Recognition*, 42, pp. 1832–1844 (2009).
[27] Povinelli, R.J., Johnson, M.T., Lindgren, A.C., Roberts, F.M. and Ye, J. "Statistical models of reconstructed phase spaces for signal classification", *IEEE Transactions on Signal Processing*, 6(54), pp. 517–526 (2006).
[28] Owis, M.I., Abou-Zied, A.H., Youssef, A.M. and Kadah, Y.M. "Study of features based on nonlinear dynamical modeling in ECG arrhythmia detection and classification", *IEEE Transactions on Biomedical Engineering*, 7(49), pp. 481–498 (2002).
[29] Tsipouras, M.G., Voglis, C. and Fotiadis, D.I. "A framework for fuzzy expert system creation-application to cardiovascular diseases", *IEEE Transactions on Biomedical Engineering*, 11(54), pp. 1181–1196 (2007).
[30] Christov, I., Jekova, I. and Bortolan, G. "Premature ventricular contraction classification by the Kth nearest-neighbours rule", *Physiological Measurement*, 26, pp. 123–130 (2006).
[31] Minhas, F.A. and Arif, M. "Robust electrocardiogram (ECG) beat classification using discrete wavelet transform", *Physiological Measurement*, 29, pp. 555–570 (2008).
[32] Exarchos, T.P., Tsipouras, M.G., Exarchos, C.P., Papaloukas, C., Fotiadis, D.I. and Michalis, L.K. "A methodology for the automated creation of fuzzy expert systems for ischaemic and arrhythmic beat classification based on a set of rules obtained by a decision tree", *Artificial Intelligence in Medicine*, 40, pp. 187–200 (2007).
[33] Christov, I. and Bortolan, G. "Ranking of pattern recognition parameters for premature ventricular contractions classification by neural networks", *Physiological Measurement*, 25, pp. 1281–1290 (2004).
[34] Polat, K., Kara, S., Güven, A. and Günes, S. "Usage of class dependency based feature selection and fuzzy weighted pre-processing methods on classification of macular disease", *Expert Systems with Applications*, 36, pp. 2584–2591 (2009).
[35] Liu, H., Sun, J., Liu, L. and Zhang, H. "Feature selection with dynamic mutual information", *Pattern Recognition*, 42, pp. 1330–1339 (2009).
[36] Abe, N. and Kudo, M. "Non-parametric classifier-independent feature selection", *Pattern Recognition*, 39, pp. 737–746 (2006).
[37] Peng, H., Long, F. and Ding, C. "Feature selection based on mutual information: criteria of max-dependency, max-relevance, and min-redundancy", *IEEE Transactions on Pattern Analysis and Machine Intelligence*, 8(27), pp. 712–724 (2005).
[38] Tsipouras, M.G., Fotiadis, D.I. and Sideris, D. "An arrhythmia classification system based on the RR-interval signal", *Artificial Intelligence in Medicine*, 33, pp. 237–250 (2005).
[39] Nilsson, M., Funk, P., Olsson, E.M.G., von Scheele, B. and Xiong, N. "Clinical decision-support for diagnosing stress-related disorders by applying psycho physiological medical knowledge to an instance-based learning system", *Artificial Intelligence in Medicine*, 36, pp. 159–176 (2006).
[40] de Chazal, P. and Reilly, R.B. "A Patient-adapting heartbeat classifier using ECG morphology and heartbeat interval features", *IEEE Transactions on Biomedical Engineering*, 12(53), pp. 1475–1486 (2006).
[41] Melgani, F. and Bazi, Y. "Classification of electrocardiogram signals with support vector machines and particle swarm optimization", *IEEE Transactions on Information Technology in Biomedicine*, 5(12), pp. 667–677 (2008).
[42] Yu, S.N. and Chou, K.T. "A switchable scheme for ECG beat classification based on independent component analysis", *Expert Systems with Applications*, 33, pp. 824–829 (2007).
[43] Ghaffari, A., Homaeinezhad, M.R., Khazraee, M. and Daevaeiha, M. "Segmentation of holter ECG waves via analysis of a discrete wavelet-derived multiple skewness–kurtosis based metric", *Annals of Biomedical Engineering,* Springer Publishing, 4(38), pp. 1497–1510 (2010).
[44] Ghaffari, A., Homaeinezhad, M.R., Akraminia, M., Atarod, M. and Daevaeiha, M.' "A robust wavelet-based multi-lead electrocardiogram delineation algorithm", *Medical Engineering & Physics*, 10(31), pp. 1219–1227 (2009).
[45] Mallat, S., *A Wavelet Tour of Signal Processing*, Academic Press (1999).
[46] Bishop Christopher, M., *Pattern Recognition and Machine Learning*, Springer Publishing (2006).
[47] Benitez, D., Gaydecki, P.A., Zaidi, A. and Fitzpatrick, A.P. "The use of the Hilbert transform in ECG signal analysis", *Computers in Biology and Medicine*, 31, pp. 399–406 (2001).
[48] Ghaffari, A., Homaeinezhad, M.R., Atarod, M. and Akraminia, M. "Parallel processing of ECG and blood pressure waveforms for detection of acute hypotensive episodes: a simulation study using a risk scoring model", *Computer Methods in Biomechanics and Biomedical Engineering*, 13(2), pp. 197–231 (2010).
[49] Homaeinezhad, M.R., Najjaran Toosi, H., Ghaffari, A., Tahmasebi, M. and Daevaeiha, M.M. "Long-duration ambulatory holter ECG QRS complex geometrical templates extraction by non-parametric clustering of the QRS virtual close-up extracted feature space", *The Proceedings of the Computing in Cardiology Conference*, Belfast, UK, pp. 937–940 (2010).
[50] Osowski, S. and Linh, T.H. "ECG beat recognition using fuzzy hybrid neural network", *IEEE Transactions on Biomedical Engineering*, 48, pp. 1265–1271 (2001).
[51] Dokur, Z., Olmez, T. and Yazgan, E. "Comparison of discrete wavelet and Fourier transforms for ECG beat classification", *Electronics Letters*, 35, pp. 1502–1504 (1999).
[52] Hu, Y.Z., Palreddy, S. and Tompkins, W.J. "A patient-adaptable ECG beat classifier using a mixture of experts approach", *IEEE Transactions on Biomedical Engineering*, 44, pp. 891–900 (1997).